

SELF HEATING OF CORONA BY ELECTROSTATIC FIELDS DRIVEN BY SHEARED FLOWS

H. Saleem¹, S. Ali², S. Poedts³

1&2. National Centre for Physics, Quaid-i-Azam University Campus,
Shahdarra Valley Road, Islamabad, Pakistan

3. K.U.Leuven, Belgium

A mechanism of self-heating of solar corona is pointed out. It is shown that the free energy available in the form of sheared flows gives rise to unstable electrostatic waves which accelerate the particles and heat them. The electrostatic perturbations take place through two processes (a) by purely growing sheared flow-driven instability and (b) by sheared flow-driven drift waves. These processes occur throughout the corona and hence the self-heating is very important in this plasma. These instabilities can give rise to local electrostatic potentials φ of the order of about 100 volts or less within 3×10^{-2} to a few seconds time if the initial perturbation is assumed to be about one percent that is $\frac{e\varphi}{T_e} \simeq 10^{-2}$. The components of wave lengths in the direction perpendicular to external magnetic field \mathbf{B}_0 vary from about 10m to 1m. The purely growing instability creates electrostatic fields by sheared flows even if the density gradient does not exist whereas the density gradient is crucial for the concurrence of drift wave instability.

Subject headings: Sun: self-heating of corona, sheared flow-driven instability, drift waves.

PACS numbers:

I. INTRODUCTION

Several theoretical models have been presented to explain the cause of solar coronal heating (Aschwanden 2001; Mandrini, Demoulin, & Klimchuk 2000). It is a well-known counter intuitive fact that the corona is 200 times hotter

than the chromosphere while it is a rarefied collision-less plasma with electron temperature $T_e \simeq 10^6(K)$. There are many puzzles in the problem of coronal heating. The temperature rises by two orders of magnitude from upper chromosphere to lower corona through a transition layer of only about 500 km (Priest 1982; Narain; Ulmschneider & Klimchuk 2006). The proposed wave heating mechanisms assume that the waves originate in the lower regions and deposit their energy in the corona. Observational data of Skylab, Yohkoh, SOHO and TRACE has indicated that the entire corona is filled with open and closed magnetic field lines and only a subset of it is loaded with hot plasma at a given time (Litwin & Rosner 1993; Hara et al. 1992; Moses et al. 1997; Schrijver et al. 1999). The coronal loops have also been considered to be responsible for localized heating.

The bright coronal loops have higher densities compared to the ambient faint coronal plasma which indicates that the heated plasma originates from the dense chromosphere. The coronal heating by acoustic waves originating from global oscillations have been ruled out (Aschwanden 2001). Alfvén waves have been considered to be the best candidate for carrying adequate energy fluxes from chromosphere to corona (Hollweg & Sterling 1994). A great deal of work on Alfvén wave heating of the corona has appeared in literature (Ionson 1983; Mok 1987; Steinolfson & Davila 1993; Ofman, Davila & Steinolfson 1995; Helberstadt & Goedbloed 1995; Ruderman et al. 1997).

Any unstable wave in this plasma can cause coronal heating through damping either by wave-particle interaction or by other linear and nonlinear mechanisms. Most of the theories pertaining to wave heating in corona are based

on magnetohydrodynamics (MHD) and hence electrostatic drift-waves have not been investigated while in fact the system itself is highly inhomogeneous. There are many suggested mechanisms for heating in which the main energy source is provided to corona by other regions.

We point out an important energy source available within the corona to excite short scale electrostatic perturbations and that are the sheared flows of plasma streams and rivers. These electrostatic perturbations can be associated with either the purely unstable mode (D'Angelo 1965) or the drift-waves of two fluid plasma depending upon the scales of density inhomogeneity and the wavelengths. Vranjes and Poedts (2009a) have proposed a new paradigm of solar coronal heating by drift waves. They have used the results of kinetic theory which predicts that drift wave is a universally unstable mode and density gradient is the source of its instability which is also the cause of its existence. It has been proposed that the drift waves can heat the corona through two possible ways, one due to the Landau damping effects in the direction parallel to the magnetic field, and another one, the stochastic heating in the perpendicular direction. It has been confirmed (De Pontieu et al. 2007) that the solar atmosphere is highly structured and has inhomogeneous density filaments of various sizes. Therefore drift waves in corona may have several different scales of wavelengths.

Vranjes and Poedts (2009a) assume external magnetic field is along z-axis while the density gradient is along x-axis and wave propagates under local approximation in yz-plane with perpendicular wavelength $\lambda_y = \frac{2\pi}{k_y}$ and parallel wavelength $\lambda_z = \frac{2\pi}{k_z}$ while $k_z \ll k_y$ (where k_y and k_z are respective

wave numbers). The drift waves have been considered with $\lambda_y \simeq 0.5m$ while $\lambda_z = 20km$ and $L_n = 100m$ (where $L_n = \left| \frac{1}{n_0} \frac{dn_0}{dx} \right|^{-1} km$) is the density gradient scale length.

We focus our attention on the fact that sheared flows are omnipresent in the corona. Thus a large source of energy for the excitation of short scale electrostatic perturbations exist within the corona. Two types of electrostatic instabilities are expected to occur throughout the corona continually:

- I. Purely growing sheared flow-driven instability in doppler shifted frame (D'Angelo 1965) which exist even if the plasma density is uniform
- II. Drift wave instability which needs plasma density gradient for it's existence (Kadomtsev & Timofeev (1963)) and sheared flows for instability (Saleem, Vranjes & Poedts (2007))

We investigate the drift waves having relatively longer wavelengths compared to ion Larmor radius so that the fluid model can be justified. Moreover, the electrons are assumed to follow Boltzmann distribution. Therefore frequencies ω_r of drift waves must fulfill the condition $\omega_r \ll \nu_{te} k_z$ where $\nu_{te} = (T_e/m_e)^{1/2}$ is the electron thermal velocity and k_z is the wave number parallel to external magnetic field. The drift waves and purely growing D'Angelo mode have shorter wavelengths compared to Alfvén waves of MHD model, in general. The electrostatic perturbations driven by sheared flows can transfer their energy to plasma particles. For the case of drift waves a detailed picture has been presented by Vranjes & Poedts (2009a). The drift dissipative instabilities have also been discussed by Vranjes & Poedts (2009b).

II. THEORETICAL MODEL

Let us consider the collisionless coronal plasma consisting of two types of ions $j = a, b$, where 'a' represents Hydrogen ions and 'b' represents Helium ions. We choose the ambient magnetic field as $\mathbf{B}_0 = B_0 \hat{\mathbf{z}} \equiv \text{constant}$, $\nabla n_{j0} = -\hat{\mathbf{x}} \left| \frac{dn_{j0}}{dx} \right|$, and the shear flow as $\nu_0(x) = v_{j0}(x) \hat{\mathbf{z}} = v_0(x) \hat{\mathbf{z}}$ where v_0 is the same for all species; electrons and both type of ions. Each species has a zero-order diamagnetic drift $\mathbf{v}_{Dj0} = -\left(\frac{T_j}{q_j B_0} \right) \nabla \ln n_{j0} \times \hat{\mathbf{z}}$ where T_j is temperature and q_j is charge of the j th species of ions. For electrostatic perturbation, the momentum equation yields the perpendicular component of the velocity of j th species of ions as,

$$\begin{aligned} \mathbf{v}_{\perp j} &= \frac{1}{B_0} (\mathbf{E}_{\perp} \times \hat{\mathbf{z}}) - \frac{T_j}{q_j B_0} (\nabla \ln n_j \times \hat{\mathbf{z}}) - \frac{1}{q_j B_0} \left(\frac{\nabla \cdot \mathbf{\Pi}_j}{n_j} \right) - \frac{1}{\Omega_j} (\partial_t + \mathbf{v}_j \cdot \nabla) \mathbf{v}_j \times \hat{\mathbf{z}} \\ &= \mathbf{v}_E + \mathbf{v}_{Dj} + \mathbf{v}_{\Pi j} + \mathbf{v}_{pj} \end{aligned} \quad (1)$$

where $\mathbf{v}_E, \mathbf{v}_{Dj}, \mathbf{v}_{\Pi j}$ and \mathbf{v}_{pj} are the electric, diamagnetic, stress tensor and polarization drifts, respectively. The parallel component of momentum equation gives,

$$(\partial_t + v_{j0z} \partial_z) v_{jz1} + v_{jz1} d_x \nu_{j0z}(x) = \frac{q_j}{m_j} E_{z1} - \frac{T_{j0}}{m_j n_{j0}} \partial_z n_{j1} \quad (2)$$

Here $d_x = \frac{d}{dx}$ and the subscripts naught (0) and one (1) denote zero order and linear quantities, respectively. The continuity equation for j th ions is,

$$\begin{aligned} (\partial_t n_{j1} + v_{j0z} \partial_z) \partial_t n_{j1} + \nabla n_{j0} \cdot \mathbf{v}_E + \frac{n_{j0}}{B_0 \Omega_j} (\partial_t + v_{j0z} \partial_z) \nabla_{\perp} \cdot \mathbf{E}_{\perp} \\ \nu_{0z} - \frac{T_j}{q_j B_0 \Omega_j} (\partial_t + \nu_{j0z} \partial_z) \nabla_{\perp}^2 n_{j1} + n_{j0} \partial_z v_{jz1} = 0 \end{aligned} \quad (3)$$

where $\Omega_j = \frac{q_j B_0}{m_j}$ and $\nabla \nu_{0z}(x) = +\hat{\mathbf{x}} \left| \frac{d\nu_0(x)}{dx} \right|$. In obtaining (3), we have used the following relation

$$\begin{aligned} \nabla \cdot [n_j (\mathbf{v}_{jp} + \mathbf{v}_{j\pi})] &= \frac{n_{j0}}{B_0 \Omega_j} \partial_t (\nabla_{\perp} \cdot \mathbf{E}_{\perp 1}) - \frac{T_j}{q_j B_0 \Omega_j} \partial_t \nabla^2 n_{j1} \\ &+ \frac{n_{j0}}{\Omega_j} v_0(x) \partial_z \left\{ \frac{1}{B_0} \nabla_{\perp} \cdot \mathbf{E}_{\perp} - \frac{T_j}{q_j B_0} \frac{\nabla_{\perp}^2 n_{j1}}{n_{j0}} \right\} \end{aligned} \quad (4)$$

The continuity equations for $j = a, b$ can also be expressed as,

$$R_a^2 n_{a1} = -n_{a0} S_a^2 \Phi_1 \quad (5)$$

$$R_b^2 n_{b1} = -n_{b0} S_b^2 \Phi_1 \quad (6)$$

where

$$\begin{aligned} R_a^2 &= (1 + \rho_{aT}^2 k_y^2) \Omega_{\omega}^2 - \nu_{te}^2 k_y^2 \\ R_b^2 &= (1 + \rho_{bT}^2 k_y^2) \Omega_{\omega}^2 - \nu_{te}^2 k_y^2 \\ S_a^2 &= \left\{ -\omega_a^* \Omega_{\omega} + \rho_{as}^2 k_y^2 \Omega_{\omega}^2 + c_{as}^2 k_y k_z \frac{1}{\Omega_a} \frac{dv_0}{dx} - c_{as}^2 k_z^2 \right\}, \\ S_b^2 &= \left\{ -\omega_b^* \Omega_{\omega} + \rho_{bs}^2 k_y^2 \Omega_{\omega}^2 + c_{bs}^2 k_y k_z \frac{1}{\Omega_b} \frac{dv_0}{dx} - c_{bs}^2 k_z^2 \right\}, \end{aligned}$$

Here we have defined $\nu_{Tj}^2 = \frac{T_{j0}}{m_j}$, $\Omega_j = \frac{q_j B_0}{m_j}$, $c_{js}^2 = \frac{T_e}{m_j}$, $\Omega_{\omega} = (\omega - \omega_0)$, $\omega_0 = v_0 k_z$,

$\omega_j^* = D_e \kappa_{jn} \kappa_y$, $\kappa_{jn} = \left| \frac{1}{n_{j0}} \frac{dn_{j0}}{dx} \right|$, and $\Phi = \frac{e\varphi}{T_e}$.

Poisson equation in this case can be written as,

$$\nabla \cdot \mathbf{E}_1 = \frac{e}{\epsilon_0} (n_{a1} + n_{b1} - n_{e1}) \quad (7)$$

and electrons (e) are assumed to follow the Boltzmann relation,

$$n_{e1} \simeq n_{e0} e^{\Phi} \quad (8)$$

In steady state the relation $n_{e0} = n_{a0} + n_{b0}$ holds. Equations (5 - 8) yields a fourth order dispersion relation as follows,

$$L_4\Omega_\omega^4 + L_3\Omega_\omega^3 + L_2\Omega_\omega^2 + L_1\Omega_\omega + L_0 = 0 \quad (9)$$

where

$$\begin{aligned} L_4 &= \Lambda^2\alpha_a^2\alpha_b^2 + \frac{n_{a0}}{n_{e0}}(\alpha_b^2\rho_{as}^2k_y^2) + \frac{n_{b0}}{n_{e0}}(\alpha_a^2\rho_{bs}^2k_y^2) \\ L_3 &= - \left\{ \frac{n_{a0}}{n_{e0}}\alpha_b^2\omega_a^* + \frac{n_{b0}}{n_{e0}}\alpha_a^2\omega_b^* \right\} \\ L_2 &= -\Lambda^2(\alpha_a^2\nu_{bT}^2k_z^2 + \alpha_b^2\nu_{aT}^2k_z^2) + \frac{n_{a0}}{n_{e0}}(\alpha_b^2g_a c_{sa}^2k_z^2 \\ &\quad - \rho_{as}^2k_y^2\nu_{bT}^2k_z^2) + \frac{n_{b0}}{n_{e0}}(\alpha_a^2g_b c_{bs}^2k_z^2 - \rho_{bs}^2k_y^2\nu_{aT}^2k_z^2) \\ L_1 &= \frac{n_{a0}}{n_{e0}}(\nu_{bT}^2k_z^2\omega_a^*) + \frac{n_{b0}}{n_{e0}}(\nu_{aT}^2k_z^2\omega_b^*) \\ L_0 &= \Lambda^2\nu_{aT}^2k_z^2\nu_{bT}^2k_z^2 - \frac{n_{a0}}{n_{e0}}g_a\nu_{bT}^2k_z^2c_{as}^2k_z^2 - \frac{n_{b0}}{n_{e0}}g_b\nu_{aT}^2k_z^2c_{bs}^2k_z^2 \end{aligned}$$

Here $g_j = \left(\frac{k_y}{k_z}A_j - 1\right)$, $A_j = \frac{1}{\Omega_j} \frac{dv_0}{dx}$, $\alpha_j^2 = (1 + \rho_{jT}^2k_y^2)$, $\lambda_{De}^2 = \frac{\epsilon_0 T_e}{n_{e0} e^2}$, and $\Lambda^2 = (1 + \lambda_{De}^2 k^2)$.

III. APPLICATION TO CORONA

Now we show that the theoretical model presented above is perfectly applicable to coronal plasma. Let us choose the parameters of the corona (Priest 1982) as $n_{e0} = 1015m^{-3}$, $n_{a0} = 0.9n_{e0}$, and $T_e = 10^6 K$. Since the condition $T_e < T_H < T_{He}$ holds in this plasma (Hansteen, Leer, and Holtzer 1997), therefore we assume $T_a = 2.5T_e$ and $T_b = 3T_e$.

First we show that the sheared flows of electron proton plasma of corona gives rise to purely growing and oscillatory drift wave instabilities. Then it

will be shown that the presence of second ion (Helium 10%) in this plasma modifies the growth rate and the real frequencies of the drift wave in different parameter regimes. If this 10% concentration of the ions in the plasma is neglected, then we may use $n_{b0} = 0$ and $T_{b0} = 0$ in the equation (9). In the limit $\lambda_{De}^2 k^2 \ll 1$, we have $\Lambda^2 = 1$, $\alpha_b^2 = 1$, $\frac{n_{a0}}{n_{e0}} = 1$, $\nu_{bT}^2 = 0$ and it gives $L_4 = \rho_{as}^2 k_y^2 + \alpha_a^2$, $L_3 = -\omega_a^*$, $L_2 = -n u_{aT}^2 k_z^2 + g_a c_{as}^2 k_z^2$ and $L_1 = 0 = L_0$. In this case equation (9) reduces to

$$(1 + \rho_{aT}^2 k_y^2 + \rho_{as}^2 k_y^2) \Omega_\omega^2 - \omega_a^* \Omega_\omega + A_a k_z c_{as}^2 - (c_{as}^2 + v_{aT}^2) k_z^2 = 0 \quad (10)$$

This quadratic equation has two roots

$$\begin{aligned} (\Omega_\omega)_{1,2} &= \frac{1}{2\Lambda_0} \left[\omega_a^* \pm \left\{ (\omega_a^*)^2 + 4\Lambda_0 c_{as}^2 k_z^2 \left((1 + \sigma_a) - A_a \frac{k_y}{k_z} \right) \right\} \right] \\ (\Omega_\omega)_{1,2} &= \frac{1}{2\Lambda_0} \left\{ \omega_a^* \pm \left[(\omega_a^*)^2 + 4\Lambda_0 c_{as}^2 k_z^2 \left((1 + \sigma_a) - A_a \frac{k_y}{k_z} \right) \right] \right\} \end{aligned} \quad (11)$$

where $\Lambda_0 = (1 + \rho_{aT}^2 k_y^2 + \rho_{as}^2 k_y^2)$. Following conditions should satisfy simultaneously for the instability.

$$(1 + \sigma_a) \frac{k_z}{k_y} < A_a \quad (12)$$

and

$$(\omega_a^*)^2 < 4\Lambda_0 c_{as}^2 k_z^2 \left| \left((1 + \sigma_a) - A_a \frac{k_y}{k_z} \right) \right| \quad (13)$$

We shall assume that κ_{nj} has the same value for all species and that can be denoted by κ_n . In Fig. 1, the growth rates of the shear flow-driven electrostatic instability are plotted using equation (10) against different gradient scale lengths of the plasma flow parallel to external magnetic field in case of homogeneous density. The real frequency in laboratory frame is ω_0 . But in

the moving frame of plasma, it is a purely growing instability and therefore ω_i has been plotted vs perpendicular wavenumber k_y . We notice that the imaginary frequency ω_i decreases corresponding to the same k_y when the shear flow gradient scale length $L_v = \frac{1}{\kappa_v}$ increases. Thus the steeper gradients give rise to larger growth rate of the instability.

In the presence of density gradient, the electrostatic drift wave can also be excited. Fig. 2 shows that the drift wave becomes unstable for $2 < k_y < 2.5$ for a very short range of wavelengths. Somewhere in between $k_y = 2$ and $k_y = 2.5$, the real frequency of drift wave ω_a^* is larger than the growth rate ω_i that is $\omega_i < \omega_a^*$ and hence linear analysis is valid. The drift wave seems to be driven by the sheared-flow. The pattern of growth rate ω_i for $2 < k_y < 2.5$ becomes different in Fig. 2 which has $\kappa_n \neq 0$ compared to Fig. 2 plotted for $\kappa_n = 0$. For $2.5 \leq k_y$, the purely growing instability dominates because here $\omega_r \ll \omega_i$ and hence it shows the shear flow-driven instability with local real frequency $\omega_0 = \nu_0 k_z$. Both ω_i and ω_r becomes larger for drift wave when the shear flow gradient is steeper as shown in Fig. 3 while the density gradient is kept constant $\kappa_n = 1.9 \times 10^{-3} m^{-1}$. We notice that the growth rates and real frequency of the drift wave decrease corresponding to smaller k_y and k_z compared to Fig. 2 which is quite natural. In this case the instabilities require larger value of flow because $c_{as}^2 k_z^2$ - term becomes smaller in condition (13). In Fig. 4, the effect of the ration of $\frac{k_z}{k_y}$ on instabilities is shown. In Fig. 5 the effect of the presence of helium ions on real and imaginary frequencies is shown on the shear flow-driven instability (for $\kappa_n = 0$) and on the drift wave instability for ($\kappa_n \neq 0$).

IV. ROLE OF DISSIPATION

The Solar corona is commonly assumed to be a collision-less plasma because most of the wave studies deal with the relatively higher frequency Alfvén waves using MHD equations or ion acoustic waves with the wave numbers larger than our regime of parameters and hence the frequency becomes larger than the electron-ion collision frequency ν_{ei} . The drift waves have been investigated in corona first time (to the best of authors knowledge) by Vranjes and Poedts (2009a) and (2009b). The drift waves investigated by Vranjes & Poedts (2009a) have frequencies $\omega_r \sim \omega_i \sim 10^2 \text{rad/s}$ and $\nu_{ei} \simeq 30 \text{rad/s}$ (Vranjes & Poedts 2009b). Therefore the ideal plasma approximation is valid. In the higher frequency (ω^*_a) regime it does not seem preferable to assume electrons to be inertia-less because the condition $\omega^*_a \ll v_{te}k_z$ may not remain valid. We choose the wave parameters such that the condition $\omega^*_a, \omega^*_b \ll v_{te}k_z$ remains valid and electrons follow the Boltzmann distribution. But here we see another small effect namely the dissipation. Let us look at the Fig. 2(a) to analyze the role of drift wave in corona. This wave is stable for $k_y < 2$ and then for $2 < k_y < 3$, the wave develops ω_i and for $3 < k_y$ we can see that $\omega_r < \omega_i$ and the shear flow-driven instability dominates. To understand the wave behaviour, we choose a value of k_y in between 2 and 3. Let $k_y = 2.2m^{-1}$, then for $\kappa_n = 1.9 \times 10^{-3}m^{-1}$ we find $\omega^*_a = D_e \kappa_n k_y \simeq 36 \text{rad/s}$ which is equal to ν_{ei} . Therefore, dissipation can play some role in this frequency regime. It is important to note that the well-known drift dissipative instability (DDI) (Weiland 2000) does not become important even in this range of frequencies because $\omega^*_a \not\ll \nu_{ei}$. The parallel momentum equation for electrons yields

(Weiland 2000)

$$\frac{n_{e1}}{n_{e0}} \simeq \frac{e\varphi}{T_e} \left\{ 1 - \nu \frac{\nu_{ei}}{\nu_{te}^2 k_z^2} (\omega_a^* - \omega) \right\} \quad (14)$$

in the limit $\omega_a^* \ll \nu_{ei}$. In ion continuity equation the limit $c_s^2 k_z^2 \ll \omega_a^*$ is used along with $n_e \simeq n_i$, to obtain linear dispersion relation for DI with the real frequency ω_{rd} and imaginary frequency ω_{id} as (Weiland 2000),

$$\omega_{rd} \simeq \frac{\omega_a^*}{(1 + \rho_{as}^2 k_y^2)} \quad (15)$$

and

$$\omega_{id} \simeq \left(\frac{\omega_r^2}{\nu_{te}^2 k_z^2} \right) \nu_{ei} \rho_{as}^2 k_y^2 \quad (16)$$

In our case, the drift wave frequency can be of the order of ν_{ei} . Since we have shown that the drift wave becomes unstable due to sheared flow in the absence of electron-ion collisions, therefore in our parameter regime, the dissipation can just add its small effect to the already unstable perturbation. But the DDI is not applicable because the real frequency ω_a^* is not much smaller than ν_{ei} .

The Fig. 2(a) indicates that for small k_y -values, the drift wave is stable and shear flow does not have an effect on it. So for longer wavelengths $k_y \ll 2$, the drift dissipative instability in corona can take place. As an example, let us choose $k_y = 0.1 m^{-1}$ and take rest of the parameters to be the same i.e. $\kappa_n = 1.9 \times 10^{-3}$, $k_z = 10^{-4} k_y$, $B_0 = 10^{-2} T$ etc. Then we find $\omega_a^* \simeq 1.63$, $\nu_{te} k_z \simeq 36$ while $\nu_{ei} \simeq 36$. Then $\omega_a^* \simeq \nu_{ei} \ll \Omega_i$ holds along with $\omega_a^* \ll \frac{\nu_{te}^2 k_z^2}{\nu_{ei}}$. Therefore, the drift dissipative instability in corona gives rise to drift waves having very low frequency $\omega_a^* \simeq 1 Hz$ and relatively longer wavelength $\lambda_y \simeq \frac{2\pi}{k_y} \simeq 60 m$.

V. DISCUSSION

It has been proposed that the large perturbed electrostatic fields are generated throughout the solar corona, due to localized sheared plasma flows, which accelerate the particles and heat them. The corona is not a static ball of plasma, rather it has flows and gradients. Therefore, it has already been proposed that the free energy available in the form of density gradients can produce electrostatic drift waves (Vranjes & Poedts 2009a, 2009b). Using the results of kinetic theory, these authors have shown that the universally unstable drift waves can heat the coronal ions very efficiently. The density gradient in the direction perpendicular to the external magnetic field is the cause of the existence of these waves as well as it is the source for their instability. The waves transfer their energy to plasma particles through Landau damping (the wave-particle interaction). This process cannot be studied using fluid models.

But the two fluid theory has predicted a Kelvin-Helmholtz type instability which takes place in plasmas because of sheared flows (D'Angelo 1965). It shows that if both electrons and ions flow with the same velocity along the external magnetic field \mathbf{B}_0 and there exists a gradient in flow in the direction perpendicular to \mathbf{B}_0 , then the perturbed electrostatic field becomes unstable. These are purely growing fields in the frame of reference of the flow wide spectrum of wavelengths. But in laboratory frame these unstable perturbations have associated local real frequencies as $\omega_0 = v_0(x)k_z$. The sheared flows in corona can give rise to two types of electrostatic instabilities continuously throughout the corona.

1. Sheared flow-driven instability (D'Angelo 1965) even if the plasma density is uniform ($\kappa_n = 0$)
2. The drift wave, which exists if the density is non-uniform $\kappa_n \neq 0$, instability due to sheared flow

These instabilities have been investigated neglecting the effects of electron-ion collisions. For $k_y \simeq 10m^{-1}$, we find that the sheared flow-driven instability can create potential $\varphi \simeq 68$ volt in about growth-time $\tau_g \simeq 0.03s$ if at $t = 0$ we assume $\frac{e\varphi}{T_e} \simeq 10^{-2}$. Note that Vranjes & Poedts (2009a) have estimated that large frequency drift waves ($\omega_r \simeq 2.5 \times 10^2$) can give rise to this value of potential in 0.02 s. The components of wavelength chosen in the perpendicular and parallel directions are, respectively, $\lambda_y = 0.5m^{-1}$ and $\lambda_z = 20km$. Then they have $\nu_{te}k_z = 1.2 \times 10^3$.

We have also shown that the drift waves having $\omega_r < 50$ rad/s satisfy $\omega_r \ll \nu_{te}k_z$ can become unstable due to sheared flow. The collisional effects have been neglected which can only modify the growth rates by small amounts. It is well-known that the electron-ion collisions can drive drift dissipative instability and it does not require plasma flow to occur. The collisions produce electrostatic drift waves having very small real frequency $\omega_{rd} \simeq 1.6$ rad/sec corresponding to $k_y \simeq 0.1m^{-1}$ and longer wavelengths $\lambda_y = \frac{2\pi}{k_y} \simeq 60m$. If the initial perturbation is assumed to be $\Phi_0 = e\frac{e\varphi}{T_e} = 10^{-2}$, then φ will take time $\tau_g \simeq 15$ minutes to grow up to $\varphi = 86$ volt. But smaller values of φ will be produced in much small times than 15 minutes. Thus we conclude that drift waves of different frequencies and wavelengths are produced in the solar corona due to sheared flows and electron-ion collisions.

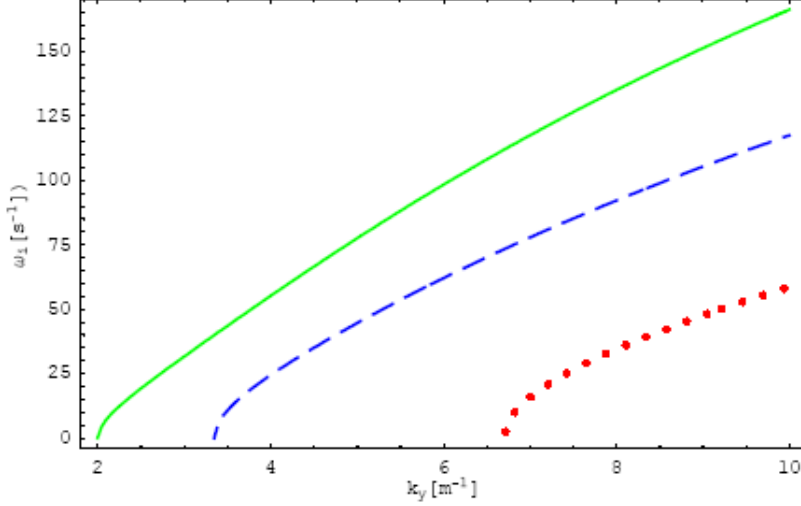


Fig .1

FIG. 1: (Color online) The growth rate (ω_i) is plotted against the perpendicular component of the wavenumber (k_y) for different inverse velocity scalelengths; $\kappa_v = k_y/60$ (solid curve), $\kappa_v = k_y/100$ (dashed curve), and $\kappa_v = k_y/200$ (dotted curve) with $n_{e0} \sim n_{a0} \sim 10^{15} \text{ m}^{-3}$, $T_e = 10^6 \text{ K}$, $T_a = 2.5 T_e$, $B_0 \sim 10^{-2} \text{ Tesla}$, $v_0 = 10 \text{ km/s}$, $\kappa_{nj} = 0$, $n_{b0} = 0$, and $k_z = 10^{-4} k_y \text{ m}^{-1}$.

Thus electrostatic fields are almost omnipresent in the coronal plasma and continuous self-heating is taking place due to sheared flows and density gradients. The present investigation shows that even if the plasma density is uniform in a region, the electrostatic fields will be produced because corona is not static and sheared flows occur everywhere. Therefore, the sheared flow driven instability plays an important role in self-heating of the corona.

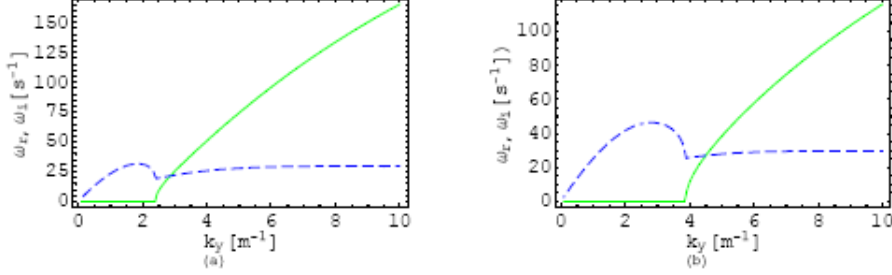


Fig. 2

FIG. 2: (Color online) The real and imaginary frequencies [ω_r (dashed curve), ω_i (solid curve)] are plotted against the perpendicular component of the wavenumber (k_y) for varying inverse velocity scalelength (a) $\kappa_v = k_y/60$, and (b) $\kappa_v = k_y/100$, taking $v_0 = 10$ km/s, $\kappa_n = 1.9 \times 10^{-3} \text{ m}^{-1}$, $n_{b0} = 0$, and $k_z = 10^{-4}k_y\text{m}^{-1}$. All other parameters are the same as in Fig.1.

Captions

Figure 6: (Color online) The imaginary and real frequencies (a) ω_i and (b) ω_r , are plotted against the perpendicular component of the wavenumber (k_y), respectively, for $n_{b0} = 0$ (dashed curve) and $n_{b0} = 0.1n_{e0}$ (solid curve), with $v_0 = 10$ km/s, $n_{e0} \sim 10^{15} \text{ m}^{-3}$, $n_{a0} \sim 0.9n_{e0}$ and $B_0 \sim 10^{-2}$ Tesla, taking $\kappa_n = 0$, $\kappa_v = k_y/60$, and $k_z = 10^{-4}k_y\text{m}^{-1}$.

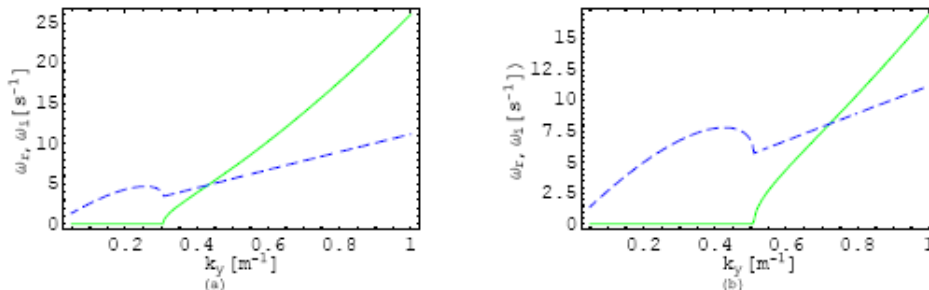


Fig. 3

FIG. 3: (Color online) The real and imaginary frequencies [ω_r (dashed curve), ω_i (solid curve)] are plotted against the perpendicular component of the wavenumber (k_y) for changing inverse velocity scalelength (a) $\kappa_v = k_y/60$ and (b) $\kappa_v = k_y/100$, keeping $v_0 = 70$ km/s, $\kappa_n = 1.9 \times 10^{-3} \text{ m}^{-1}$, $n_{b0} = 0$, and $k_z = 10^{-4} k_y \text{ m}^{-1}$. All other parameters are the same as in Fig.1.

Aschwanden, M.J. 2001, ApJ, 560, 1035, 1044.

A.Rogava, Z.Osmanov, and S.Poedts: “Self-heating as a possible cause of the chromospheric heating in solar-type stars”, MNRAS 404, 224, 2010. doi:10.1111/j.1365-2966.2009.16159.x

B. M. Shergelashvili, S. Poedts, A. D. Pataraya, “Non-modal self-heating of the solar atmosphere: an alternative way to enhance the wave heating process”, Proc. SPM-11: ‘The Dynamic Sun: Challenges for Theory and Observations’, Leuven, Belgium, 11-16 September 2005, D. Danesy, S. Poedts, A. De Groof, J. Andries (eds.), ISBN 92-9092-911-1, ISSN 1609-042X, ESA SP-600 (Dec. 2005) 4p.

B. M. Shergelashvili, S. Poedts, A. D. Pataraya: “The non-modal cascade in the compressible solar atmosphere: self-heating – an alternative way to enhance wave heating”, ApJL642, L73, 2006.

De Pontieu et al, Science, 2007, 318, 1574

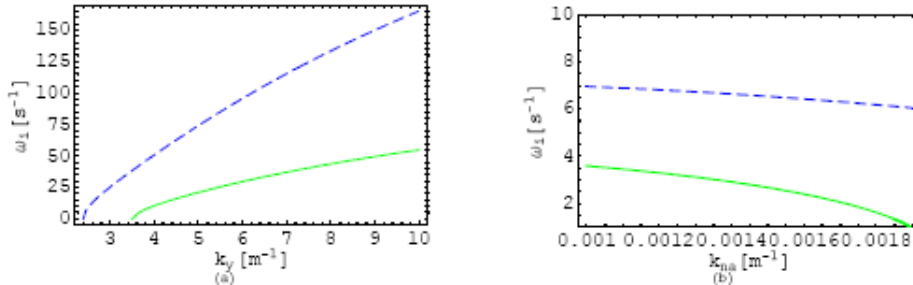


Fig. 4

FIG. 4: (Color online) The growth rate ω_i is plotted against the perpendicular component of the wavenumber (k_y) and the inverse density scalelength (κ_n), respectively, varying the parallel component of the wavenumber (a) $k_z = 10^{-5}k_y\text{m}^{-1}$ (solid curve), $k_z = 10^{-4}k_y\text{m}^{-1}$ (dashed curve) with fixed values of $v_0 = 10\text{ km/s}$, $\kappa_n = 1.9 \times 10^{-3}\text{ m}^{-1}$, and $\kappa_v = k_y/60$, and the streaming velocity (b) $v_0 = 50\text{ km/s}$ (solid curve), $v_0 = 70\text{ km/s}$ (dashed curve), with $\kappa_v = k_y/60$, $k_y = 0.5\text{ m}^{-1}$, and $k_z = 10^{-4}k_y\text{m}^{-1}$. All other parameters are the same as in Fig.1.

D'Angelo, N. 1965, Phys. Fluids, 8, 1748

Halberstadt, G. & Goedbloed, J.P., 1995, A & A, 301, 559.

Hara, H., Tsuneta, S., Lemen, J.R., ACton, L.W. & Mc Tiernan, J.M. 1992, PAS J, 44, L135.

Hollweg, J.V. & Sterling, A.C. 1994, ApJ, 282, L31.

Ionson, J.A., 1983, ApJ, 271, 778,.

Kadomtsev, B.B., & Timofeev, A.V. 1963, Sov. Phys. Doklady, 7, 826.

Klimtchuk, J.A., 2006, Solar Phys. 234, 41.

Litwin, C. & Rosner, R. 1993, ApJ, 412, 375.

Mandrini, C.H., Demoulin, P. & Klimchuk, J.A. 2000, ApJ, 530, 999.

Mok, Y. 1987, A & A, 172, 327.

Moses, D., et al. 1997, Sol. Phys., 175, 571.

Narain, U. Ulmschneider, P., 1990, Space Sci. Rev., 54, 377.

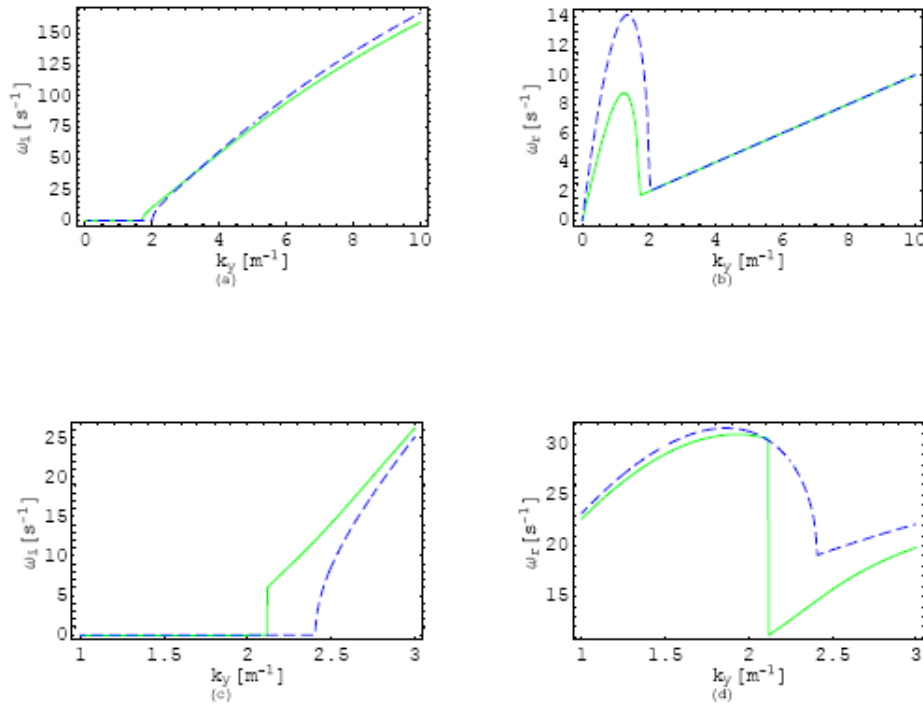


Fig. 5

FIG. 5: (Color online) The imaginary and real frequencies (a) ω_i and (b) ω_r , are plotted against the perpendicular component of the wavenumber (k_y), respectively, for $n_{b0} = 0$ (dashed curve) and $n_{b0} = 0.1n_{e0}$ (solid curve), with $v_0 = 10$ km/s, $n_{e0} \sim 10^{15}$ m $^{-3}$, $n_{a0} \sim 0.9n_{e0}$ and $B_0 \sim 10^{-2}$ Tesla, taking $\kappa_n = 1.9 \times 10^{-3}$ m $^{-1}$, $\kappa_v = k_y/60$, and $k_z = 10^{-4}k_y$ m $^{-1}$.

Ofman, L., Davila, J.M. & Steinolfson, R.S. 1995, ApJ, 444, 471.

Priest, E.R., 1982, Solar Magnetohydrodynamics (England, D. Reidel Publishing Company), 7.

Ruderman, M.S., Berghmans, D. Goossens, M. & Poedts, S., 1997, A & A, 320, 305.

Saleem, H., Vranjes, J., & Poedts, S., 2007, A&A, 471, 289.

Schrijver, C.J., et al. 1999, Sol. Phys., 187, 261.

Steinolfson, R.S. & Davila, J. 1993, ApJ, 415, 354.

Vranjes, J. & Poedts, S. 2009a, EPL, 86, 39001.

Vranjes, J. & Poedts, S., 2009b, *Mon. Not. R. Astron. Sol.*, 398, 918.